J. Chem. Sci. (2019)131:83
https://doi.org/10.1007/s12039-019-1660-3

REGULAR ARTICLE

A simple Schiff base platform: sensing of Al^{3+} ions in an aqueous medium

RAJASEKARAN DHIVYA, ASAITHAMBI GOMATHI and PERIASAMY VISWANATHAMURTHI*
Department of Chemistry, Periyar University, Salem, Tamilnadu 636 011, India
E-mail: viswanathamurthi@gmail.com

MS received 23 April 2019; revised 21 June 2019; accepted 25 June 2019

Abstract. A simple Schiff base probe **PADP** ((1,2-phenylenebis(azanylylidene)) bis(methanylylidene))bis(3-(diethylamino)phenol) was synthesized from 4-(diethylamino)salicylaldehyde and *o*-phenylenediamine and has been characterized using analytical and spectral methods. The emission spectrum of **PADP** Schiff base shows notable enhancement in the emission intensity at 500 nm in the presence of Al^{3+} in MeOH-H_2O (1:9 v/v). On the other hand, other relevant metal ions did not influence considerably the emission spectrum of **PADP**. The detection limit and binding constant (K_b) of **PADP** towards Al^{3+} were found to be 0.104 μM and 3.0 × 10^6 M^{-1} from the fluorescence titration experiments. The 1:1 binding stoichiometry was further determined by Job's plot and ESI-MS spectroscopy. The MTT assay shows no or negligible toxic nature of probe and thus it was utilized *in vitro* cell imaging studies of Al^{3+} ions. The results show that the probe **PADP** could be useful to detect Al^{3+} in an aqueous medium.

Keywords. Schiff base; fluorescence probe; aluminum ion; cell imaging.

1. Introduction

Aluminum is one of the most widely used and abundant metal in the earth's crust and 8.1% of the crust contains Aluminum. It is commonly used to manufacture electrical equipment, automobiles, building construction, water purification, clinical drugs,[1] packaging materials,[2] etc. It is neither toxic nor essential to the human body. But unregulated amounts of aluminum in the human body may lead to damage to the central nervous system. The diseases such as dementia, loss of memory, listlessness, severe trembling, Parkinson's,[3] Alzheimer's[4,5] and dialysis[6] are caused due to the increased amount of aluminum in the human body. An even higher concentration of aluminum is toxic to plant growth and aquatic fishes.[7–9] Hence, the presence of aluminum ions has been strictly regulated in drinking water and surface water by the Environmental Protection Agency (EPA). Thus selective and sensitive detection method of aluminum ions becomes very much necessary. In recent years, researchers focused on recognition of metal ions by using fluorescent chemosensor. The use of fluorescent chemosensor is not only an inexpensive method but it also has advantages like high sensitivity, short response time and facilitated detection to identify the metal ions when compared to other sophisticated utensils like AAS, ICP-MS, etc.[10–17] Even though a plethora of receptors were reported for the detection of Al^{3+},[18–24] it is still worthwhile to design ratiometric and colorimetric fluorescent probes that detect Al^{3+}. The design of chemosensors for Al^{3+} is difficult due to its small size (53.5 pm) and high charge (+3). Moreover, Al^{3+} undergoes strong binding with H_2O, which significantly decreases its ligand coordination ability in an aqueous medium. However, hard centers like O may be suitably arranged to bind an Al^{3+} ion due to its hard acid nature.

Based on the above information, a simple N_2O_2 Schiff base fluorescent probe has been designed and synthesized by the condensation reaction of 4-(diethylamino)salicylaldehyde and *o*-phenylenediamine.

*For correspondence

Electronic supplementary material: The online version of this article (https://doi.org/10.1007/s12039-019-1660-3) contains supplementary material, which is available to authorized users.

Published online: 28 August 2019

The sensor has been developed based on photoinduced electron transfer (PET) mechanism. When lone pairs of electrons on the imine nitrogen or oxygen atoms are used for coordination, then these electrons are no longer available to quench the emission intensity of the probe, thereby increasing the fluorescence intensity. The fluorescence 'off–on' sensing phenomenon caused by Al^{3+} was demonstrated by fluorescence, UV-Vis, mass spectrometry and NMR studies and was also proved in the cellular medium using NCCS cells.

2. Experimental

2.1 *Materials and methods*

All chemicals were purchased from Sigma-Aldrich and commercially available analytical grade solvents were used without further purification. Fresh double distilled water was used throughout the experiments. Melting points were checked on a Technico micro heating table and are uncorrected. Analytical data were obtained using Vario EL III Elemental analyzer. UV-Visible and fluorescence spectra were recorded on Shimadzu 1800 and JASCO FP-8200 spectrophotometer respectively using a 1 cm square quartz cell in DMSO–H_2O (1:9 v/v) HEPES buffer solution (pH 7.4). ^{1}H-NMR spectra were measured in DMSO-d_6 or $CDCl_3$ on a Bruker AMX-500 spectrometer at 400 MHz. The chemical shifts (δ) recorded in ppm with reference to tetramethylsilane (TMS). Electrospray ionization mass spectra (ESI-mass) were collected on an advanced Q-TOF micro^{TM} mass spectrometer. Cell imaging was done on the (Eclipse Ti-U, Nikon, USA) fluorescence microscope.

2.2 *Synthesis of ((1,2-phenylenebis(azanylylidene)) bis(methanylylidene))bis(3-(diethylamino)phenol) (PADP)*

4-(Diethylamino)salicylaldehyde (0.7724 g, 4 mmol) and *o*-phenylenediamine (0.2162 g, 2 mmol) were added in ethanol (20 mL) and the mixture was refluxed at 80 °C for 12 h. The progress of the reaction was monitored by TLC (Thin Layer Chromatography). After completion, the reaction mixture was cooled to room temperature and the solvent was evaporated. The orange color precipitate formed was purified by column chromatography using petroleum ether/ethyl acetate (8:2) mixture as eluent.

Yield (60% 0.52 g): M.p.: 90 °C. Elemental analysis for $C_{28}H_{34}N_4O_2$: C, 73.33; H, 7.47; N, 12.22%. Found: C, 73.28; H, 7.42; N, 12.17; %. FT-IR (v/cm^{-1}): 2963 (-OH group), 1604 (CH=N), UV-vis (MeOH, λ_{max}, nm): 352,378. ^{1}H NMR ($CDCl_3$, ppm): 9.5 (s, 2H), 8.4 (s, 2H), 6–7.5 (m, J = 7.21 Hz, 10H), 3.5–4.0 (q, J = 7.6 Hz 8H), 1.2–1.5(t, J = 7.42 Hz 12H) (Figure S1, Supplementary Information) MS (ESI, *m/z*): 459.5 $[M+H]^+$. (Figure S2, Supplementary Information).

2.3 *Synthesis of aluminum complex (PADP-Al^{3+})*

The receptor **PADP** (0.458g, 1 mmol) and aluminum nitrate nonahydrate (0.3751 g, 1 mmol) were dissolved in ethanol (20 mL) and the mixture was stirred under the room temperature for 3 h. The green coloured precipitate formed was filtered and washed with cold ethanol.

Yield: 84%, 0.61g; M.p.: 300 °C above. Anal.Calc for $C_{28}H_{34}N_5AlO_6$: C, 59.67; H, 6.08; N, 12.43%. Found: C, 59.17; H, 5.58; N, 11.93. FT-IR (v/cm^{-1}): 1504 (CH=N), UV-Vis [DMSO, λ_{max}, nm]: 376, 410. ^{1}H NMR (DMSO-d_6 ppm): 8.6 (s, 2H), 5.5–7.5 (d, J = 7.2 Hz, 10H) 3.5–4.0 (q, J = 7.41 Hz, 8H), 1.3–1.5 (t, J = 7.46 Hz, 12H) (Figure S3, Supplementary Information), MS (ESI, *m/z*): 561.1 $[M-H]^+$.

3. Results and Discussion

The simple Schiff base compound **PADP** was synthesized by a single step using 4-(diethylamino)salicylaldehyde and *o*-phenylenediamine in ethanol (Scheme 1). The formation of the compound was confirmed by analytical and spectral techniques such as FT-IR, UV-vis, ^{1}H NMR and ESI-MS.

3.1 *UV-Vis spectroscopic studies of PADP in the presence of Al^{3+}*

The cation recognition property of the probe **PADP** was primarily studied by absorption spectra. The absorption spectrum of free **PADP** shows intense bands positioned at 352 and 378 nm which may be attributed to the intramolecular charge transfer (CT) transition. The absorption spectra of probe **PADP** with various important metal ions like Li^+, Na^+, K^+, Co^{2+}, Ni^{2+}, Mn^{2+}, Zn^{2+}, Ag^+, Ca^{2+}, Mg^{2+}, Cu^{2+}, Cd^{2+}, Hg^{2+}, Pb^{2+}, Al^{3+} and Fe^{3+} in HEPES buffer in DMSO: H_2O (1:9 v/v) medium were recorded. As shown in Figure 1, no appreciable changes in absorption were observed during the addition of metal ions with **PADP** except Al^{3+} ion. When Al^{3+} ion was added to the **PADP** probe solution, peak at 352 nm was shifted to 376 nm (redshift) with increasing intensity. Simultaneously, the band at 378 shifted to 410 nm (redshift) with decreasing intensity. During the addition of Al^{3+} ion, the color of the receptor solution changed from brownish yellow to greenish-yellow. The color change was visible to the naked eye under a UV lamp. This observation indicates that Al^{3+}

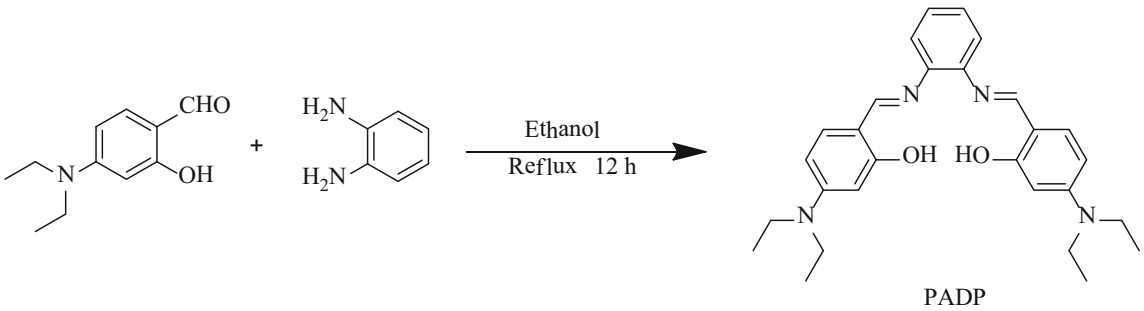

Scheme 1. The synthetic route of **PADP**.

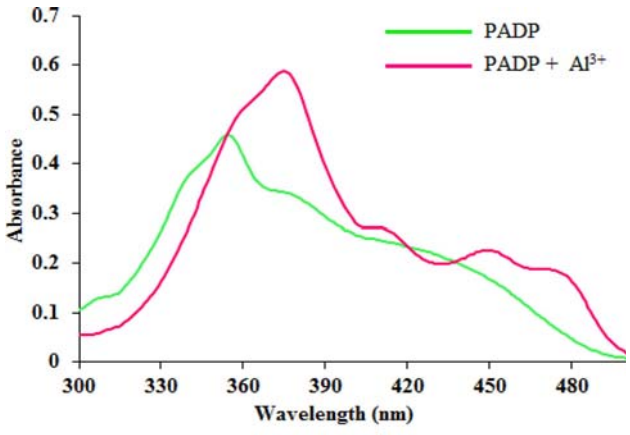

Figure 1. UV-Vis Spectra of the probe PADP (10μM) in MeOH/H_2O (1:9 (v/v), HEPES = 50mM, pH = 7.4) and with 100 μM of Al^{3+} metal ion.

ion interacts specifically with probe over the other metal ions. Besides, to find out the strength and extent of binding of Al^{3+} ions with receptor, UV-Vis titrations were done. It was carried out by the gradual addition of a standard solution of Al^{3+} ions (0–100 μM) to the solution of **PADP** (10 μM). The results show that the absorption band intensity was gradually increased at 376 nm (Figure S4, Supplementary Information) accompanied by redshift and reach a maximum at 100 μM.

In addition, the reversibility of the **PADP**-Al^{3+} complex was also performed by the addition of stronger chelating agent EDTA (ethylenediaminetetraacetate) by using absorption study. The absorption spectrum shows that the **PADP**-Al^{3+} complex was completely reversed when the treatment of EDTA (Figure S5, Supplementary Information).

3.2 *Fluorescence spectral studies*

To find the binding ability of **PADP** towards Al^{3+}, fluorescence emission study was carried out in HEPES buffer in MeOH:H_2O (1:9) medium. The probe **PADP** shows very weak emission at 500 nm (λ_{ex} = 450 nm). After confirming the fluorescence property of **PADP**, its sensing capability was tested. On the addition of various metal cations (Ag^+, Mg^{2+}, Cu^{2+}, Co^{2+}, Ni^{2+}, Mn^{2+}, K^+, Zn^{2+}, Cd^{2+}, Ca^{2+}, Hg^{2+}, Pb^2 and Al^{3+}) to the **PADP**, no significant fluorescence enhancement was observed at 500 nm except in the case of Al^{3+} ions. The addition of Al^{3+} ions caused a clear and prominent enhancement in the emission intensity at λ_{max} 500 nm (Figure 2). The enhancement in fluorescence intensity could be due to the strong binding of Al^{3+} ion to **PADP** because of the formation of a chelate ring through which CHEF (chelation enhanced fluorescence) mechanism.

To examine the binding affinity of **PADP** towards Al^{3+} ions further, the fluorescence titration experiment was carried out for **PADP** with the increasing quantity of Al^{3+} ions (Figure 3). The emission intensity of **PADP** was gradually increased with the increasing amount of Al^{3+} ion (0–100 μM). The fluorescence intensity at 500 nm and Al^{3+} concentration show a

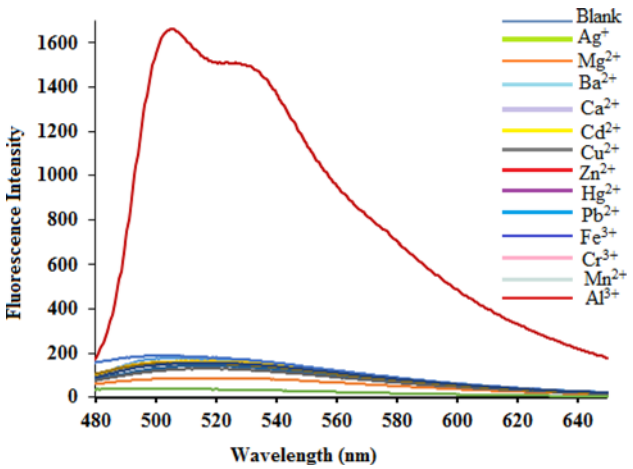

Figure 2. Fluorescence response of probe PADP (10 μM) in MeOH/H_2O (1:9 (v/v), HEPES = 50 mM, pH = 7.4) with 100 μM of metal ions (Ag^+, Mg^{2+}, Ba^{2+}, Ca^{2+}, Cd^{2+}, Cu^{2+}, Zn^{2+}, Mn^{2+}, Hg^{2+}, Pb^{2+}, Fe^{3+}, Cr^{3+} and Al^{3+}) (λ_{ex} = 450 nm).

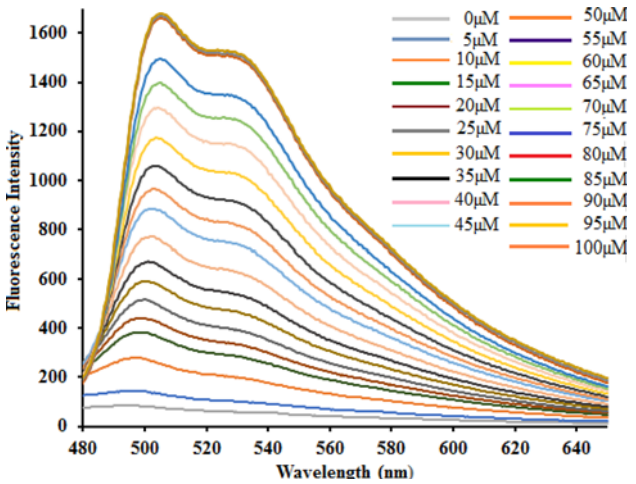

Figure 3. Fluorescence response of the probe PADP (10 μM) in MeOH/H_2O (1:9 (v/v), HEPES = 50 mM, pH = 7.4) with 0–100 μM of Al^{3+} (λ_{ex} = 450 nm).

linear relationship over the range of 0–100 μM and this indicates that the probe **PADP** is very much suitable for quantitative recognition of Al^{3+} ions. The limit of detection (LOD) of Fe^{3+} was measured to be 0.104 μM according to the (3σ/slope) method (Figure 4), which is lower than most of the previously reported Al^{3+} sensors (Table S1, Supplementary Information). The association constant (K_b) was calculated from the fluorescence titration experiment by using the Benesi-Hildebrand equation (Figure S6, Supplementary Information) and the value was measured to be 3.0×10^6 M^{-1}. The low detection limit and high binding constant value show that **PADP** could be an effective fluorogenic sensor for the detection of Al^{3+} ions.

Furthermore, the fluorescence emission spectrum of PADP-Al^{3+} complex with EDTA was recorded to check the reversibility and the corresponding results were depicted in Figure S7, Supplementary

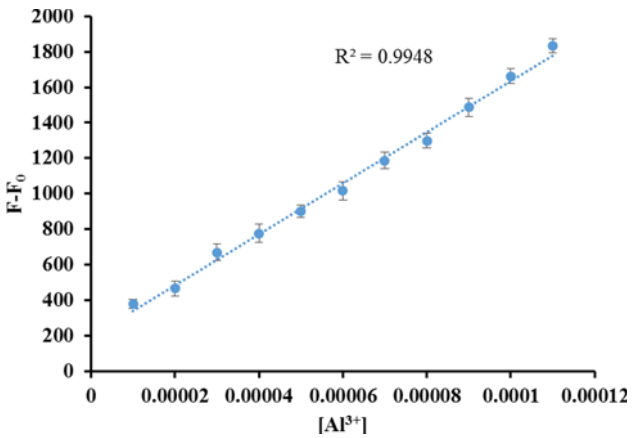

Figure 4. Calibration curve between emission intensity and concentration of aluminum ions.

Information. From the results, it was noted that the emission intensity of PADP-Al^{3+} complex was completely quenched at 500 nm, upon addition of EDTA. Simultaneously, fluorescence titration experiment was conducted with the increasing amount of EDTA (0–70 μM). The emission intensity was gradually decreased with the addition of an increasing quantity of EDTA. Finally, the fluorescence intensity was unchanged, which is identical to the emission spectrum of **PADP** (Figure S8, Supplementary Information). The results reveal that the PADP-Al^{3+} complex formation is completely reversible with EDTA. After establishing the binding of **PADP** with Al^{3+} ions, the Job's plot drawn from fluorescence titration data was utilized for binding stoichiometry (Figure S9, Supplementary Information). It can be seen that maximum value is found at the mole fraction of 0.5 indicating 1:1 binding stoichiometry.

The formation of **PADP**-Al^{3+} complex was further confirmed by spectral (IR, ^{1}H-NMR and ESI mass) studies. The IR spectrum of the aluminum complex has been examined in comparison with that of the **PADP**. The spectrum of free probe showed an intense band in the 1,604 cm^{-1} characteristic of the C=N imine group. This band shifted towards lower frequencies 1,564 cm^{-1} in probe aluminum complex indicates coordination of probe with aluminum through azomethine nitrogens. The band appeared at the region 2,963 cm^{-1} in the probe spectrum was due to the stretching frequency of two phenolic OH groups. This band disappeared in **PADP** aluminum complex shows that the binding of phenolic oxygen with metal *via* deprotonation.

In the ^{1}H NMR spectrum of the probe, a singlet appeared at 9.5 ppm was assigned to phenolic OH groups. This band is not found in the spectrum of probe aluminum complex, which is consistent with deprotonation of the probe upon metal coordination. The spectrum of the probe has shown a peak for azomethine protons (–CH=N–) at 8.4 ppm, which is shifted slightly to the downfield and appeared at 8.6 ppm in probe aluminum complex, confirms the coordination of probe with aluminum through azomethine nitrogens. Moreover, peaks due to methylene and methyl groups also appeared in the expected region (Figure 5). Furthermore, the mass spectrum of **PADP**-Al^{3+} ensemble exhibited the molecular ion peak at m/z, 561.1 which was assigned to $[PADP + Al^{3+} + NO_3 + H_2O]^+$confirms the formation of **PADP**-Al^{3+} complex (Figure S10, Supplementary Information).

To evaluate the activity of newly designed probe, selectivity and interference are two important

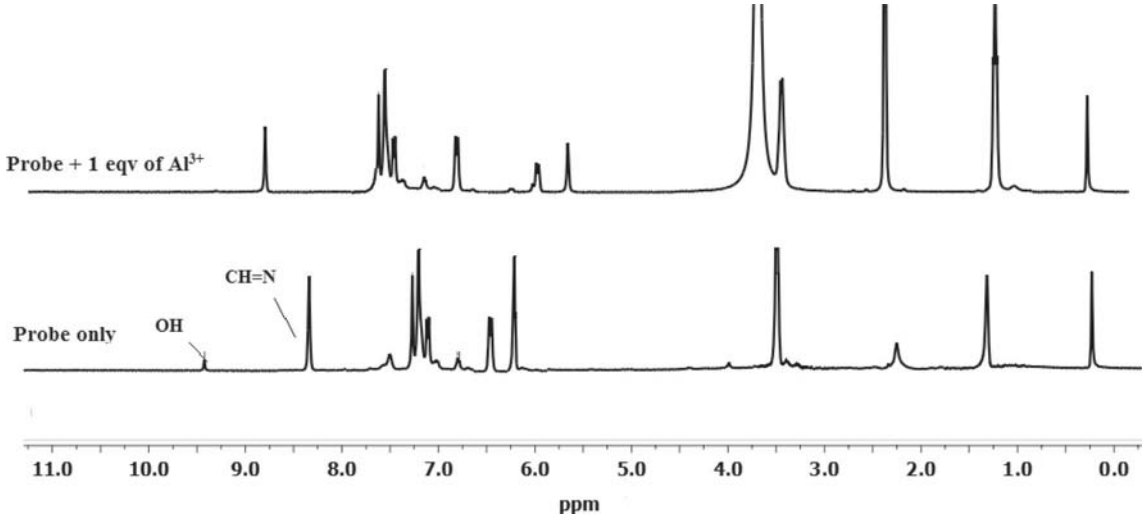

Figure 5. ^{1}H NMR spectra of probe PADP with Al^{3+} ions.

parameters. A selective response towards the target over various competing species is needed. Therefore, the selectivity study of probe to Al^{3+} over various metal ions (K^{+}, Ag^{+}, Ca^{2+}, Mg^{2+}, Cu^{2+}, Co^{2+}, Ni^{2+}, Mn^{2+}, Zn^{2+}, Cd^{2+}, Hg^{2+}, Pb^{2} and Fe^{3+}) was conducted. Moreover, interference from all above metal ions with the Al^{3+} detection by the probe was also investigated. The fluorescence results (Figure 6) show that most of the metal ions did not interfere with the detection of Al^{3+} ion by the probe **PADP**. Therefore, the probe shows excellent selectivity and interference for Al^{3+} detection among the above mentioned metal ions.

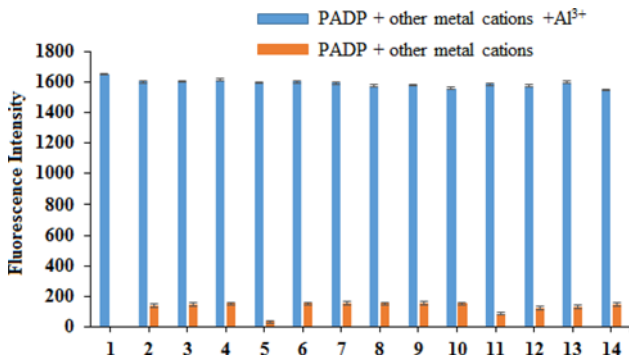

Figure 6. Relative fluorescence of ligand PADP and its complexation with Al^{3+} in the presence of various metal ions. Response of Al^{3+} was included as controls. [1. PADP + Al^{3+} + K^{+}, 2. PADP + Al^{3+} + Na^{+}, 3. PADP + Al^{3+} + Ni^{2+}, 4. PADP + Al^{3+} + Cu^{2+}, 5. PADP + Al^{3+} + Zn^{2+}, 6. PADP + Al^{3+} + Fe^{3+}, 7. PADP + Al^{3+} + Li^{+}, 8. PADP + Al^{3+} + Mg^{2+}, 9. LPADP + Al^{3+} + Cd^{2+}, 10. PADP + Al^{3+} + Hg^{2+}, 11. PADP + Al^{3+} + Pb^{2+}, 12. PADP + Al^{3+} + Cr^{3+}, 13. PADP + Al^{3+} + Mn^{2+}, 14. PADP + Al^{3+} + Ag^{+}] (left to right). Conditions: PADP, 10 μM; $Al^{3+,}$ 10 equiv.; other metal ions, 10 equiv.

To test the practical utilization of probe under physiological medium, the emission spectra of **PADP** and **PADP**-Al^{3+} ensembles were recorded under different pH condition (1–14). The results show that the receptor **PADP** could respond to the detection of Al^{3+} ions in 4–9 pH range (Figure S11, Supplementary Information) which is ideal for any biological application.

Based on the above spectroscopic results, a possible mechanism for **PADP**-probe to sense Al^{3+} ions has been proposed in Scheme 2.

3.3 *Detection of Al^{3+} ions in water samples*

The sensing property of the probe **PADP** for the determination of the spiked amount of Al^{3+} ions in river water and tap water samples were performed. The collected river water and tap water samples are spiked with different concentration levels of Al^{3+} ions (2, 4 and 6 μM). The results are shown in (Table S2, Supplementary Information) which indicate that the recovered amount of Al^{3+} ions are in good agreement with the spiked value of Al^{3+} ions. From the results, it is confirmed that the probe **PADP** detect the Al^{3+} in real samples with high accuracy.

3.4 *Detection of Al^{3+} in living cells*

Based on its encouraging fluorescence properties, **PADP** probe was exposed for biological fluorimetric detection, *in vitro* cell imaging-based recognition using NCCS cells. Before cell imaging studies, cytotoxicity of **PADP** up to 250 μM concentration was

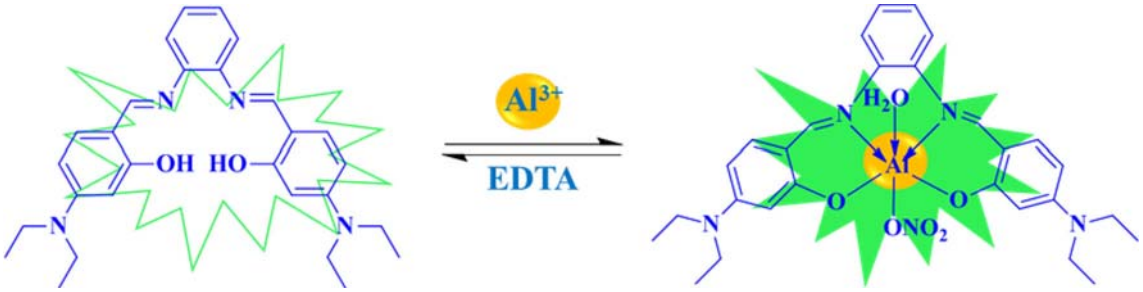

Scheme 2. Plausible mechanism for PADP-probe to sense aluminum ion.

investigated on living NCCS cells by MTT assays. The results indicate that **PADP** does not impose high cytotoxicity on the cells even at 250 μM concentration (Figure S12, Supplementary Information). Therefore, cell imaging studies were done using the non-toxic probe **PADP** by fluorescence microscopy. Owing to the weak fluorescence nature, the probe does not exhibit any substantial fluorescence when NCCS cells were incubated with 10 μM of the probe (Figure S13, Supplementary Information). When the cells were treated with 20 μM solution of Al^{3+} ions, cell fluorescence turned "ON" which is imaged through a fluorescence microscope. This result reveals that the probe **PADP** is cell-permeable and quantitatively applicable for detecting Al^{3+} ions through the formation of intracellular **PADP**-Al^{3+} complex in living cells.

4. Conclusions

A simple Schiff base chemosensor was derived from condensation between 4-(diethylamino)salicylaldehyde and *o*-phenylenediamine moieties and has been characterized using analytical and spectral methods. The emission spectrum of **PADP** Schiff base shows significant enhancement in the emission intensity at 500 nm in the presence of Al^{3+} in MeOH-H_2O (1:9 (v/v) HEPES buffer, pH 7.4). The detection limit and binding constant (K_b) of **PADP** towards Al^{3+} were found to be 0.104 μM and 3.0×10^6 M^{-1} from the fluorescence titration experiments. The 1:1 binding stoichiometry was further determined by Job's plot and further established from ESI-MS spectroscopy. The probe is found to be biocompatible as it possesses none or negligible cytotoxicity. The **PADP** was utilized *in vitro* cell imaging studies.

Supplementary Information (SI)

Experimental procedure for cell culture, cytotoxicity assay, cell imaging, ^{1}H NMR spectrum of PADP (Figure S1), Mass spectrum of PADP (Figure S2), ^{1}H NMR spectrum of PADP with Al^{3+} (Figure S3), UV-Vis titration for PADP with Al^{3+} (Figure S4), UV-Vis reversibility with EDTA (Figure S5), Benesi-Hilderbrand plot for calculating binding constant (Figure S6), fluorescence reversibility plot (Figure S7), fluorescence reversibility titration (Figure S8), Job's plot (Figure S9), mass spectrum of PADP with Al^{3+} (Figure S10), pH study (Figure S11), cytotoxicity assay (Figure S12), cell imaging (Figure S13), comparison table (Table S1) and real water sample analysis (Table S2) are available at www.ias.ac.in/chemsci.

Acknowledgement

The authors express their sincere thanks to the Council of Scientific and Industrial Research (CSIR), New Delhi, India [Grant No. 01(2907)/17/EMR-II] for financial support.

References

1. Soni M G, White S M, Flamm W G and Burdock G A 2001 Safety evaluation of dietary Aluminum *Regul. Toxicol. Pharm.* **33** 66
2. Banks W A and Kastin A J 1989 Aluminum-induced neurotoxicity: Alterations in membrane function at the blood-brain barrier *Neurosci. Biobehav. Rev.* **13** 47
3. Good P F, Olanow C W and Perl D P 1992 Neuromelanin-containing neurons of the substantia nigra accumulate iron and aluminum in Parkinson's disease: A LAMMA study *Brain Res.* **593** 343
4. Kawahara M, Muramoto K, Kobayashi K, Mori H and Kuroda Y 1994 Aluminum promotes the aggregation of Alzheimer's amyloid β-protein *in vitro Biochem. Biophys. Res. Commun.* **198** 531
5. Paik S R, Lee J H, Kim D H, Chang C S and Kim J 1997 Aluminum-induced structural alterations of the precursor of the non-Aβ component of Alzheimer's disease amyloid *Arch. Biochem. Biophys.* **344** 325
6. Lin J L, Kou M T and Leu M L 1996 Effect of long-term low-dose aluminum-containing agents on hemoglobin synthesis in patients with chronic renal insufficiency *Nephron* **74** 33
7. Delhaize E and Ryan P R 1995 Aluminum toxicity and tolerance in plants *Plant Physiol.* **107** 315

8. Rouphael Y, Cardarelli M and Colla G 2015 Role of arbuscular mycorrhizal fungi in alleviating the adverse effects of acidity and aluminium toxicity in zucchini squash *Sci. Hortic.* **188** 97
9. Poleo A B S, Ostbye K, Oxnevad S A, Andersen R A, Heibo E and Vollestad L A 1997 Toxicity of acid aluminum-rich water to seven freshwater fish species: A comparative laboratory study *Environ. Pollut.* **96** 129
10. Han T, Feng X, Tong B, Shi B J, Chen L, Zhi J G and Dong Y P 2012 A novel ''turn-on'' fluorescent chemosensor for the selective detection of Al^{3+} based on aggregation-induced emission *Chem. Commun.* **48** 416
11. Sen S, Mukherjee T, Chattopadhyay B, Moirangthem A, Basu A and Marek J 2012 A water soluble Al^{3+} selective colorimetric and fluorescent turn-on chemosensor and its application in living cell imaging *Analyst* **137** 3975
12. Kim S, Noh J Y, Kim K Y, Kim J H, Kang H K and Nam S W 2012 Salicylimine-based fluorescent chemosensor for aluminum ions and application to bioimaging *Inorg. Chem.* **5** 3597
13. Jeyanthi D, Iniya M, Krishnaveni K and Chellappa D 2013 A ratiometric fluorescent sensor for selective recognition of Al^{3+} ions based on a simple benzimidazole platform *RSC Adv.* **3** 20984
14. Upadhyay K K and Kumar A 2010 Pyrimidine based highly sensitive fluorescent receptor for Al^{3+} showing dual signalling mechanism *Org. Biomol. Chem.* **8** 4892
15. Santhi S, Amala S and Basheer S M 2018 Experimental and computational investigation of highly selective dual-channel chemosensor for Al(III) and Zn(II) ions: Construction of logic gates *J. Chem. Sci.* **130** 153
16. Chowdhury A R and Banerjee P 2017 A simple hydrazine based molecule for selective detection of Fluorideion in DMSO *J. Chem. Sci.* **129** 463
17. Yun D, Chae J B and Kim C 2019 A novel benzophenone-based colorimetric chemosensor for detecting Cu^{2+} and F^{-} *J. Chem. Sci.* **131**10
18. Peng H, Shen K, Mao S, Shi X, Xu Y, Aderinto S O and Wu H 2017 A highly selective and sensitive fluorescent turn-on probe for Al^{3+} based on naphthalimide Schiff base *J. Fluoresc.* **27** 1191
19. Tian J, Yan X, Yang H and Tian F 2015 A novel turn-on Schiff-base fluorescent sensor for aluminum(III) ions in living cells *RSC Adv.* **5** 107012
20. Lu Y, Huang S, Liu Y, He S, Zhao L and Zeng X 2011 Highly selective and sensitive fluorescent turn- on chemosensor for Al^{3+} based on a novel photoinduced electron transfer approach *Org. Lett.* **13** 5274
21. Chang Y J, Hung P J, Wan C F and Wu A T 2014 A highly selective fluorescence turn-on and reversible sensor for Al^{3+} ion *Inorg. Chem. Commun.* **39** 122
22. Wang G Q, Qin J C, Li C R and Yang Z Y 2015 A highly selective fluorescent probe for Al^{3+} based on quinoline derivative *Spectrochim. Acta A* **150** 21
23. Dong Y, Liu T, Wan X, Pei H, Wu L and Yao Y 2017 Facile one-pot synthesis of bipyridine based dual-channel chemosensor for the highly selective and sensitive detection of aluminum ion *Sensor Actuat. B Chem.* **241** 1139
24. Tang L, Ding S, Zhong K, Hou S, Bian Y and Yan X 2017 A new 2-(2′- hydroxyphenyl)quinazolin-4(3H)-one derived acylhydrazone for fluorescence recognition of Al^{3+} *Spectrochim. Acta A* **174** 70